Accurate Transfer Function Identification Based on a Dynamic Mathematical Model of Digital Steering System

HaoXin Zheng, Hongbin Liu, Peiyao Liu

Abstract—**During the launch process of an electromagnetic shell, all parts of the steering system need to bear the impact of the high-intensity instantaneous acceleration and real-time change of the system operation parameters. These problems affect the dynamic characteristics of an actuator system against overload and accurate position tracking. In this study, the dynamic mathematical model of a digital steering gear servo control system is established. A segmented error PID control method is proposed to analyze the dynamic characteristics of the actuator. The results help verify the accuracy of segmented error PID control method for analyzing the dynamic characteristics of the system. Subsequently, an electric actuator test system is designed and the step response and frequency characteristics of the actuator system are tested. Based on the experiment/least square method, the transfer function of the servo system is identified and compared with that of the simulation model; further, the accuracy of the identified transfer function is verified. This paper presents a novel method for accurately predicting the transfer function of the actuator system.**

Index Terms—**visual-steering system, PID control method, least square method, transfer function**

I. Introduction

THE actuator system of an electromagnetic projectile is important in flight control systems as it controls the flight course of missiles [1-4]. The reliability of the flight control system and the accuracy of the projectile trajectory strongly depend on the dynamic characteristics and control accuracy of the actuator system. However, the internal components of the steering gear are complex. Hence, the dynamic characteristics of each component affect the actuator; thus, it is difficult to obtain an accurate transfer function of the actuator via theoretical modeling. Therefore, this paper proposes a method to obtain a precise servo system model and the transfer function of the electric actuator.

In view of the requirements such as excellent performance, high accuracy, and small error of the actuator flight system, a few researchers have conducted dynamic mathematical modeling of the actuator system. These models optimized the dynamic characteristics of the actuator system and improved the control accuracy. He [5] proposed a complete design scheme for the TMS320F28335 DSP servo controller, which simulated the dynamic characteristics of the established mathematical model for the electric actuator control system, and elaborated the control strategy. Zhou [6] built a mathematical model for the key parameters reflecting the performance of the actuator system, which evaluated the changing trend of the failure parameters. This model provided an effective theoretical basis for predicting the slow failure of an electric actuator. Zhang [7] proposed an automatic test method for frequency characteristics and completed the small error system identification of the dynamic model of the electric actuator. Ma [8] used the parameter identification tool of MATLAB and its electric servo system to conduct identification experiments on the open-loop models of each loop of the electric servo system model. This model can realize the parameter identification of each loop of the steering gear system. Wang [9] proposed a composite control strategy combined with an adaptive controller and feed forward compensation controller. The servo system model on-line identification time-varying parameters were realized by combining the recursive least square (RLS) method of self-adjusting forgetting factor and the neural network. Sun [10] designed a test platform for the frequency response characteristics of a steering gear. A subspace identification method is used to identify the mathematical model of the steering gear. Yang [11] established a mathematical model for each component of the electric actuator system. The transfer function model of the entire steering system was obtained. Zhang [12] proposed a method of frequency characteristics test and identified the model of the electric actuator system. Wu [13] developed an improved adaptive genetic algorithm (IAGA) for the system identification. The method has the characteristics of high optimization accuracy and strong anti noise ability. It has important value in engineering application. Maarif [14] proposed a controller with integrator and state feedback, which realized the stability of the system under different reference signals and improved the system identification ability. Kharchenko [15] used harmonic detection method

Manuscript received July 28, 2020; revised February 25, 2021. This stud y was supported by the Project of Hunan Science and Technology, China (Grant No. 2016RS4056)

HaoXin Zheng is a student in Institute of Mechanical and Electronical Engineering, Central South University, Changsha, 411201, China (corresponding author phone: 029-89257667; e-mail: zhenghaoxin321@163.com)

Hongbin Liu is an engineer in Xi'an Aerospace Precision Electromechanical Research Institute, Xi'an ,710100, China（e-mail: 305736504@qq.com）

Peiyao Liu is an engineer in Xi'an Aerospace Precision Electromechanical Research Institute, Xi'an, 710100, China（e-mail: 184354327@qq.com）

and volterra transfer function model to discuss the stochastic resonance effect of nonlinear devices.

According to the above review, most scholars primarily obtained the transfer function of the steering gear system using a numerical model. However, they neglected the influence of factors such as complex working conditions of the steering gear, which led to an inaccurate identification the transfer function. To solve the aforementioned problem, this paper proposes the identification of the steering system transfer function through experiments, to realize accurate control of flight trajectory. System identification determines the model equivalent to the actual system characteristics through the input and output data of the tested system. The logic is to obtain a model through an algorithm, such that it best fit the characteristics of the system reflected by the input and output data of the tested system under the identification criteria [16]. Identification methods are increasingly abundant due to the wide application of servo control system in several fields and the continuous development of various identification algorithms. At present, the system identification methods mainly include impulse response identification [17], step response identification [18], least square identification [19], and maximum likelihood identification [20]. In addition, there are gradient identification [21], mufti-innovation identification [22], hierarchical identification [23], and other relatively new identification methods. An identification technology is required to estimate the mathematical model and parameters of the tested system through experimental data. Hence, system identification has been applied in various fields. The state equation or transfer function of the system can be obtained via system identification and modeling, and the design of a system controller can be realized.

In this study, a control model of the servo control system of the digital steering gear is established, and the mechanical characteristics of the steering gear system are simulated and analyzed using the piece wise error PID control algorithm. The overall performance test of the steering gear system is also completed, including the step response characteristics and frequency characteristics. Based on the dynamic mathematical model of the rudder system, the transfer function of the missile rudder system is identified by the least squares method.

Π. SYSTEM DYNAMIC MODELING AND CONTROL METHOD

2.1 Digital steering system

Digital actuator is a closed loop position control system and comprises a motor, mechanical transmission mechanism, sensor, and digital controller. After receiving the steering command from the electromagnetic missile system, the digital rudder compares the control deviation with the current rudder position angle. The control signal is calculated by a certain algorithm. It makes the motor rotate according to the predetermined form. The position angle of the rudder blade is corrected by the reducer to reach the predetermined position. In our work, through current feedback, speed feedback and position feedback to control the steering gear, it makes the steering gear run more stable. Fig.1 is the schematic diagram of control principle of the digital steering gear.

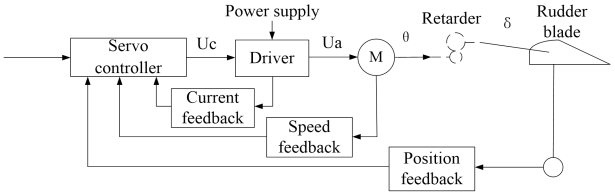

Fig.1 Control principle block diagram of digital steering gear

The steering gear is a servo system with high stability requirements. Hence, for satisfying the acquirement, it is necessary to simplify the structure of the steering gear to improve the reliability and maintainability of the steering gear. In this study, a DSP digital controller is used as the main control device, enabling easy application of different control algorithms. Through this research and comparison of control strategies, a better control effect is obtained, laying the foundation for follow-up research.

2.2 Dynamic mathematical model of steering gear system

The mathematical model block diagram of the digital steering gear is shown in Fig. 2, and includes the control algorithm, driver, motor model, and reducer model. Simulation is used to realize the simulations of various control algorithms, and the main control chip TMS320F2812 is programmed to complete the design of the steering gear.

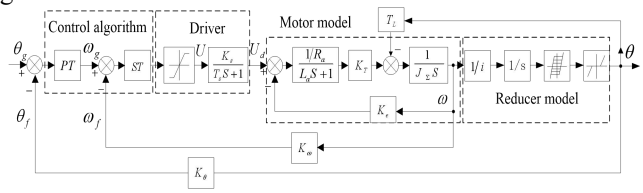

Fig. 2 Mathematical model block diagram of digital steering gear

The working environment of the actuator is complex, including nonlinear factors, and some system parameters that vary with external parameters. Hence the control strategy and control algorithm are vital to the performance of the actuator. The digital actuator is a position control servo system. The common control strategies are position loop control and position acceleration loop control.

Advancements in control theory led to the development of various control algorithms. The common algorithms are the traditional PID control, sectional error PID control, fuzzy control, and neural network control. Since the digital steering system requires an accurate position tracking strategy, the piece wise error PID control algorithm was selected in this study. The segmented error PID control [24] is based on the absolute value of the position error; thus, different control parameters are used to achieve segmented situation control of the steering gear. The block error PID control algorithm structure is displayed in Fig.3.

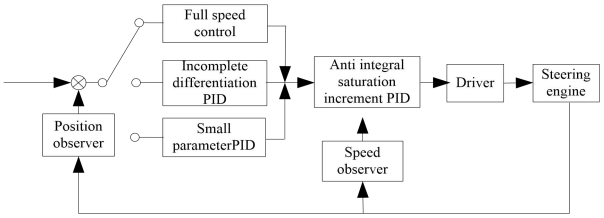

Fig.3 Block error PID control algorithm structure

(1) When the position error is in the error adjustment range $0 < e(t) < D$, the system PID parameter selects a smaller value.

(2) When the position error is in the interval $D < e(t) < G$, the system performs well using an appropriate control algorithm.

(3) When the position error is large, $G < e(t)$, the control quantity adopts full scale output. The duty cycle of pulse width modulation signal is 100%, which enables the system to rapidly compensate for the position error.

The segment error simulation is shown in Fig.4.The input deviation is divided into three segments, and the corresponding PID correction parameters of each segment are obtained through multiple simulations.

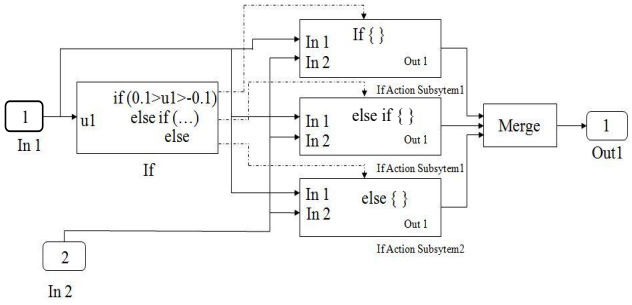

Fig.4 Simulation diagram of segmented error algorithm

(1) When the system control input deviation is within the small error range $0° \le |e(t)| \le 0.2°$, the PID parameters of the system position ring are KPP = 5000, KPI = 2500, KPD = 50, and the PI parameters of the speed ring are KSP = 10 and Ksi = 5; the proportional parameters of the current ring are Kip = 1.

(2) When the system error is in the range $0.2° < |e(t)| \le 5°$, an incomplete differential PID control algorithm is adopted. The PID parameters of the system position loop are KPP = 50000, KTI = 100, and KTD = 0.001; the PI parameters of the speed loop are KSP = 100 and Ksi = 50; and the proportional parameter of the current loop is Kip = 1.

(3) When the position error is large, $5° < |e(t)|$, the control quantity adopts full-scale output.

The dynamic mathematical model of the steering gear system is established, as shown in Fig. 5, according to the segmented error PID control method. In this study, the maximum swing angle, step characteristics, and frequency characteristics of the digital actuator are studied to verify the accuracy of the mathematical model. The steering gear system elastic load is set to 15 N·m.

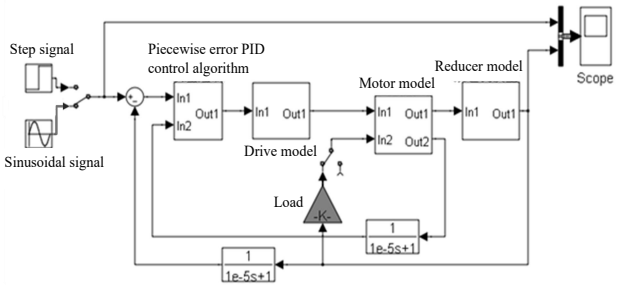

Fig.5 The simulation model of segmented error PID control for steering gear

Fig.6 shows the simulation results of the segmented error control with a 5° step signal as the input. The feedback signal delay of the steering gear system is 1ms, the rise time is approximately 35ms, the system performance follows the input step signal, and the feedback curve has no distortion. Fig. 7 shows the simulation results of segmented error control of sinusoidal signal with input amplitude of 20° and frequency of 1Hz. Fig.7 shows that the feedback signal maximum steering angle of the steering gear system is 20°, and the curve has no distortion and an obvious phase shift. Fig. 8 is the simulation result of the segmented error control of the input sinusoidal signal of amplitude 2° and frequency 13Hz. Fig.8 shows that the maximum rudder deflection feedback value of the steering gear system feedback signal is 1.9°, and the feedback curve is undistorted. Fig.9 shows the simulation results of the Bode diagram of the steering gear system.When the frequency is 98.7Hz, the amplitude represents- 3dB and the phase angle displays - 76.6 °.

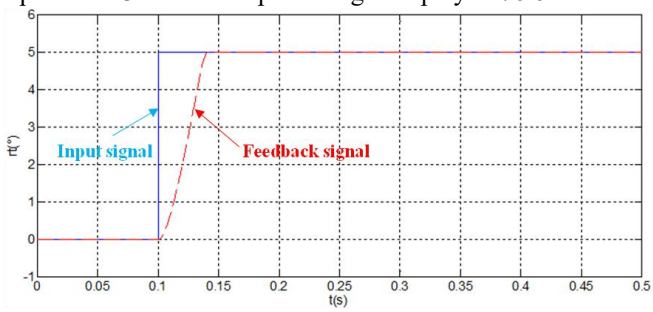

Fig.6 Simulation results of segmented error control with 5° step signal input

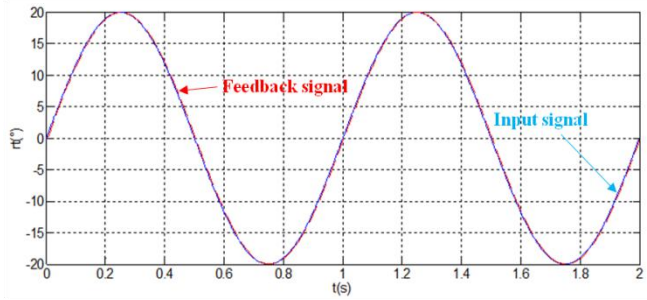

Fig.7 Simulation results of segmented error loop control for sinusoidal signals with input signal amplitude of 20° and frequency of 1Hz

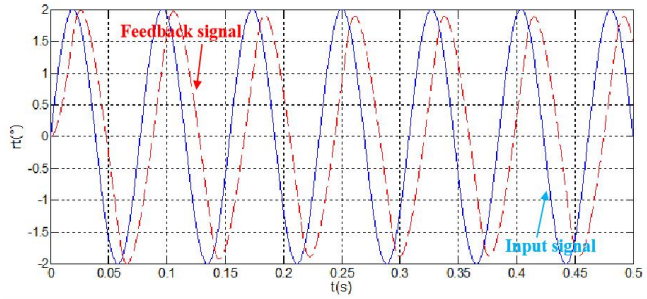

Fig.8 Simulation results of segmented error loop control for sinusoidal signals with input signal amplitude of 2° and frequency of 13 Hz

III. Experimental Test System of the Digital Steering Gear

The identification of the digital steering control system transfer function is the most important part of establishing a digital actuator test system. The inverse transfer function precisely controls the system error of the electromagnetic

actuator and ensures the position accuracy of the electromagnetic projectile.

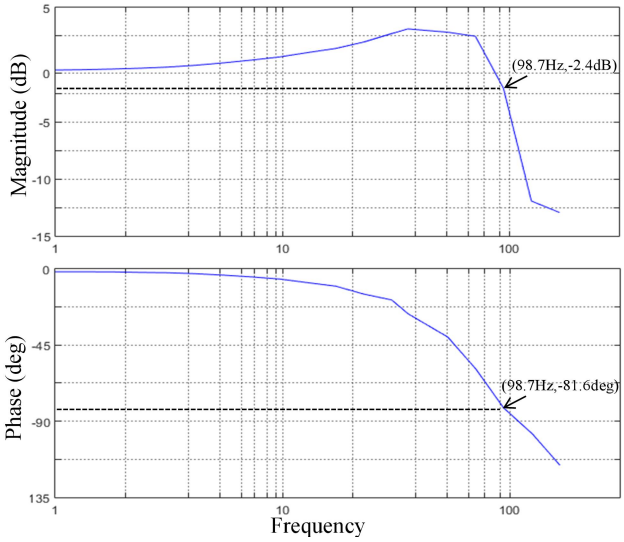

Fig. 9 Simulation results of Bode diagram of steering gear system

System identification includes experimental design, data acquisition and prepossessing, model set selection, model parameter estimation, and model verification. The basic steps of identification are shown in Fig. 10. The general process is as follows. The model structure and the identification algorithm to be used are determined according to the purpose of system identification and prior knowledge. Then, the parameters of the model are obtained through the identification algorithm using the input signal and measured output data in the experiment. Finally, the model and algorithm are varied until the identification model satisfies the requirements.

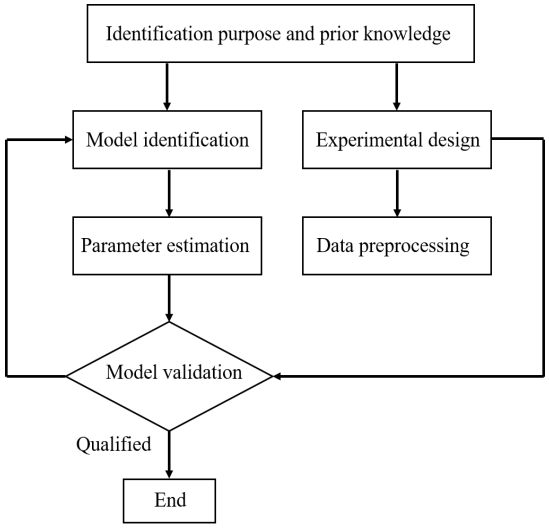

Fig. 10 Basic steps of system identification

3.1 System least square identification method

The least squares identification method is effective to study linear parameter systems and is a basic parameter estimation method for system identification. The least squares method was proposed by Gauss and has been commonly used in the field of system identification. To obtain the appropriate parameter estimation value, such that the real system output and the model output are nearly equal under the same input, the degree of proximity is judged by the sum of squares of the difference between the system output and the corresponding model output. When the sum of squares is the smallest, the corresponding parameter is the estimated value, which is the principle of the least square identification method. The controlled auto regressive model has the following forms, as shown in Eq. (1):

$$A(z)y(k) = B(z)u(k) + v(k) \tag{1}$$

$w(k) = v(k)$ present white noise, and the convergence rate of recursive least square identification algorithm for car system is studied [35], when $n = n_a + n_b$, and k<0, $y(k) = 0$, $u(k) = 0$, $v(k) = 0$, information vector and parameter vector are defined, as shown in Eq. (2) and Eq. (3):

$$\boldsymbol{\theta} = [a_1, a_2, \cdots, a_{n_a}, b_1, b_2, \cdots, b_{n_b}]^T \tag{2}$$

$$\boldsymbol{\varphi}(k) = [-y(k-1), -y(k-2), \cdots, -y(k-n_a), u(k-1), u(k-2), \cdots, u(k-n_b)]^T \tag{3}$$

Eq. (3) is expanded and moved.When k=1, 2,…, k, from the above formula, we can obtain k equations, which are written in the form of matrix:

The above formula can be abbreviated as:

$$\boldsymbol{Y}_k = \boldsymbol{H}_k\boldsymbol{\theta} + \boldsymbol{V}_k \tag{4}$$

Criteria function is defined as：

$$J(\boldsymbol{\theta}) = \boldsymbol{V}_k^T\boldsymbol{V}_k = (\boldsymbol{Y}_k - \boldsymbol{H}_k\boldsymbol{\theta})^T(\boldsymbol{Y}_k - \boldsymbol{H}_k\boldsymbol{\theta}) \tag{5}$$

Let $\boldsymbol{\theta}$ estimate be $\hat{\boldsymbol{\theta}}$, let $J(\boldsymbol{\theta})$ partial $\boldsymbol{\theta}$ derivative of the pair be 0, Eq. (6) can be obtained.

$$\frac{\partial J(\boldsymbol{\theta})}{\partial \boldsymbol{\theta}}\Big|_{\theta=\hat{\theta}} = -2\boldsymbol{H}_k^T(\boldsymbol{Y}_k - \boldsymbol{H}_k\boldsymbol{\theta})\Big|_{\theta=\hat{\theta}} = \boldsymbol{\theta}$$

$$(\boldsymbol{H}_k^T\boldsymbol{H}_k)\hat{\boldsymbol{\theta}} = \boldsymbol{H}_k^T\boldsymbol{Y}_k$$

$$\hat{\boldsymbol{\theta}} = (\boldsymbol{H}_k^T\boldsymbol{H}_k)^{-1}\boldsymbol{H}_k^T\boldsymbol{Y}_k = [\sum_{i=1}^{k}\boldsymbol{\varphi}(i)\boldsymbol{\varphi}^T(i)]^{-1}[\sum_{i=1}^{k}\boldsymbol{\varphi}(i)y(i)] \tag{6}$$

The parameters are estimated using Eq. (3). This method is also known as the one-time complete least square method, which is the off-line identification algorithm of the least square method [25-26]. When on-line identification is required, for every k, the inverse of the matrix needs to be calculated using Eq. (3); further, when the dimension of $\boldsymbol{\theta}$ is large, a corresponding number of computations are required. The RLS algorithm can avoid the matrix inversion operation, thus effectively improving the calculation efficiency. Let the estimation of the k-time parameter be $\hat{\boldsymbol{\theta}}(k)$. Then, the principle of the RLS algorithm is that the estimation of $\hat{\boldsymbol{\theta}}(k)$ at k-time parameter is equal to the estimation of $\hat{\boldsymbol{\theta}}(k-1)$ at the previous time plus a correction term [27]. A matrix is defined in Eq. (7):

$$\boldsymbol{P}^{-1}(k) = \boldsymbol{H}_k^T\boldsymbol{H}_k = \sum_{i=1}^{k}\boldsymbol{\varphi}(i)\boldsymbol{\varphi}^T(i) = \sum_{i=1}^{k-1}\boldsymbol{\varphi}(i)\boldsymbol{\varphi}^T(i) + \boldsymbol{\varphi}(k)\boldsymbol{\varphi}^T(k) \tag{7}$$

This is a symmetric, non-decreasing matrix. The above formula can be written as a recursive calculation:

$$\boldsymbol{P}^{-1}(k) = \boldsymbol{P}^{-1}(k-1) + \boldsymbol{\varphi}(k)\boldsymbol{\varphi}^T(k) \tag{8}$$

Further calculation is available

$$\boldsymbol{P}^{-1}(k)=\boldsymbol{P}^{-1}(0)+\sum_{i=1}^{k}\boldsymbol{\varphi}(i)\boldsymbol{\varphi}^{T}(i)=\boldsymbol{P}^{-1}(0)+\boldsymbol{H}_{k}^{T}\boldsymbol{H}_{k} \quad (9)$$

Compared to Eq. (1), the initial value $\boldsymbol{P}^{-1}(0)$ should be taken as a zero matrix. For practical applications, $\boldsymbol{P}^{-1}(0)$ can be considered as a relatively small positive definite matrix, $\boldsymbol{P}^{-1}(0)=\boldsymbol{I}/p_0$, and p_0 is a large normal number. Let $p_0=10^6$, we obtain $\boldsymbol{P}(0)=p_0\boldsymbol{I}$, according to the definition of $\boldsymbol{H}_k$ and $\boldsymbol{Y}_k$, and from Eq. (6), Eq. (10) is obtained.

$$\hat{\boldsymbol{\theta}}(k)=(\boldsymbol{H}_k^T\boldsymbol{H}_k)^{-1}\boldsymbol{H}_k^T\boldsymbol{Y}_k=\boldsymbol{P}(k)\boldsymbol{H}_k^T\boldsymbol{Y}_k=\boldsymbol{P}(k)\begin{bmatrix}\boldsymbol{H}_{k-1}\\ \boldsymbol{\varphi}^T(k)\end{bmatrix}^T\begin{bmatrix}\boldsymbol{Y}_{k-1}\\ y(k)\end{bmatrix}$$

$$=\boldsymbol{P}(k)[\boldsymbol{P}^{-1}(k-1)\boldsymbol{P}(k-1)\boldsymbol{H}_{k-1}^T\boldsymbol{Y}_{k-1}+\boldsymbol{\varphi}(k)y(k)]$$

$$=\hat{\boldsymbol{\theta}}(k-1)+\boldsymbol{P}(k)\boldsymbol{\varphi}(k)[y(k)-\boldsymbol{\varphi}^T(k)\hat{\boldsymbol{\theta}}(k-1)] \quad (10)$$

Eq. (5) and Eq. (6) are used to obtain the RLS algorithm of the parameter $\boldsymbol{\theta}$. To avoid the inverse operation of $\boldsymbol{P}(k)$, a lemma of matrix is introduced, let $\boldsymbol{A}\in R^{n\times n}$, $\boldsymbol{B}\in R^{n\times r}$, $\boldsymbol{C}\in R^{r\times n}$, when the matrix $\boldsymbol{A}$ and $(\boldsymbol{I}+\boldsymbol{C}\boldsymbol{A}^{-1}\boldsymbol{B})$ are invertible,

$$(\boldsymbol{A}+\boldsymbol{B}\boldsymbol{C})^{-1}=\boldsymbol{A}^{-1}-\boldsymbol{A}^{-1}\boldsymbol{B}(\boldsymbol{I}+\boldsymbol{C}\boldsymbol{A}^{-1}\boldsymbol{B})^{-1}\boldsymbol{C}\boldsymbol{A}^{-1}$$

It can be applied to Eq. (8), we can get:

$$\boldsymbol{P}(k)=\boldsymbol{P}(k-1)-\frac{\boldsymbol{P}(k-1)\boldsymbol{\varphi}(k)\boldsymbol{\varphi}^T(k)\boldsymbol{P}(k-1)}{1+\boldsymbol{\varphi}^T(k)\boldsymbol{P}(k-1)\boldsymbol{\varphi}(k)}$$

To simplify the expression, let $\boldsymbol{L}(k)=\boldsymbol{P}(k)\boldsymbol{\varphi}(k)$,

$$\boldsymbol{L}(k)=\boldsymbol{P}(k-1)\boldsymbol{\varphi}(k)-\frac{\boldsymbol{P}(k-1)\boldsymbol{\varphi}(k)\boldsymbol{\varphi}^T(k)\boldsymbol{P}(k-1)\boldsymbol{\varphi}(k)}{1+\boldsymbol{\varphi}^T(k)\boldsymbol{P}(k-1)\boldsymbol{\varphi}(k)}$$

$$=\boldsymbol{P}(k-1)\boldsymbol{\varphi}(k)[1-\frac{\boldsymbol{\varphi}^T(k)\boldsymbol{P}(k-1)\boldsymbol{\varphi}(k)}{1+\boldsymbol{\varphi}^T(k)\boldsymbol{P}(k-1)\boldsymbol{\varphi}(k)}]$$

$$=\frac{\boldsymbol{P}(k-1)\boldsymbol{\varphi}(k)}{1+\boldsymbol{\varphi}^T(k)\boldsymbol{P}(k-1)\boldsymbol{\varphi}(k)}$$

According to the formula above, the RLS algorithm of CAR model can be written as:

$$\hat{\boldsymbol{\theta}}(k)=\hat{\boldsymbol{\theta}}(k-1)+\boldsymbol{L}(k)[y(k)-\boldsymbol{\varphi}^T(k)\hat{\boldsymbol{\theta}}(k-1)] \quad (11)$$

$$\boldsymbol{L}(k)=\frac{\boldsymbol{P}(k-1)\boldsymbol{\varphi}(k)}{1+\boldsymbol{\varphi}^T(k)\boldsymbol{P}(k-1)\boldsymbol{\varphi}(k)} \quad (12)$$

$$\boldsymbol{P}(k)=\boldsymbol{P}(k-1)-\boldsymbol{L}(k)[\boldsymbol{P}(k-1)\boldsymbol{\varphi}(k)]^T \quad (13)$$

Among them, $\boldsymbol{P}(0)=p_0\boldsymbol{I}$, $p_0=10^6>>1$. The initial value of $\hat{\boldsymbol{\theta}}(0)$ can be a very small real vector, such as, $\hat{\boldsymbol{\theta}}(0)=\boldsymbol{I}_n/p_0$.

The flow chart for the parameter estimation of $\hat{\boldsymbol{\theta}}(k)$ by the RLS algorithm is shown in Fig. 11. The calculation steps of the algorithm are as follows:

(1) Let k = 1, and let the initial value of covariance matrix $\boldsymbol{P}(0)=p_0\boldsymbol{I}$, and the initial value of parameter estimation $\hat{\boldsymbol{\theta}}(0)=\frac{\boldsymbol{1}_n}{p_0}$, where, $p_0=10^6$;

(2) When k = 1, the input and output data are $u(k)$ and $y(k)$ respectively are obtained. The information vector is formed as $\boldsymbol{\varphi}(k)$;

(3) The gain matrix $\boldsymbol{L}(k)$ is calculated using Eq. (12), and the parameter estimation vector $\hat{\boldsymbol{\theta}}(k)$ is refreshed by Eq. (11);

(4) Refresh the covariance matrix $\boldsymbol{P}(k)$ through Eq. (13):

(5) Change k to k+1 and go back to the second step for the next recursive calculation.

For different system models, the least square identification algorithm can be modified to obtain the corresponding identification algorithm, such as the recursive least-squares identification method for the equation error model [28] and least square identification algorithm for auxiliary variables used to identify systems with colored noise interference.

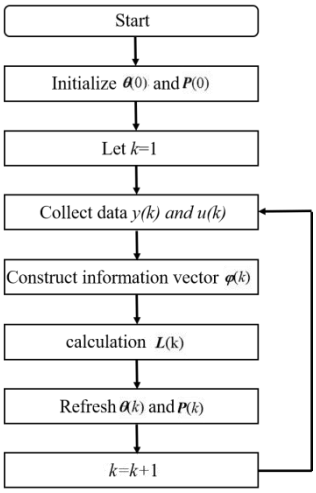

Fig. 11 The flow of RLS algorithm for parameter estimation of $\hat{\boldsymbol{\theta}}(k)$

3.2 Experimental test and analysis

During the test, the upper computer test program converts the specified input signals into control instructions, which are sent to the steering gear controller via serial communication. The controller uses the algorithm written by itself to analyze and calculate the internal control signals according to the received action instructions and drives the steering gear through the driving circuit to make corresponding action responses. Simultaneously, the potentiometer inside the actuator collects the rudder deviation signal and sends it to the controller. The controller sends these rudder deflection signals back to the upper computer through the serial port according to the transmission format set in the communication protocol. The upper computer converts the received data into the output signal for the graphic display and data processing (calculation of selected characteristics or system parameter identification, etc.). A schematic of the test system is shown in Fig. 12. The steering gear test system is shown in Fig. 1.

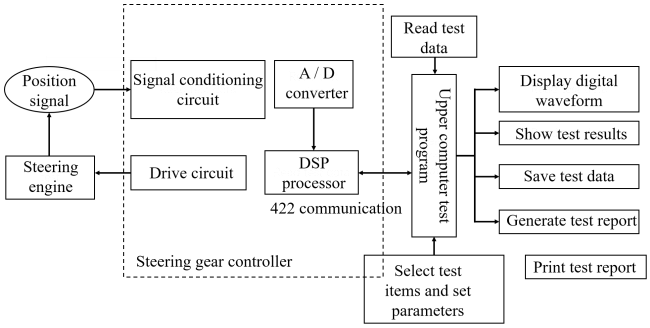

Fig. 12 Working principle diagram of steering gear test system

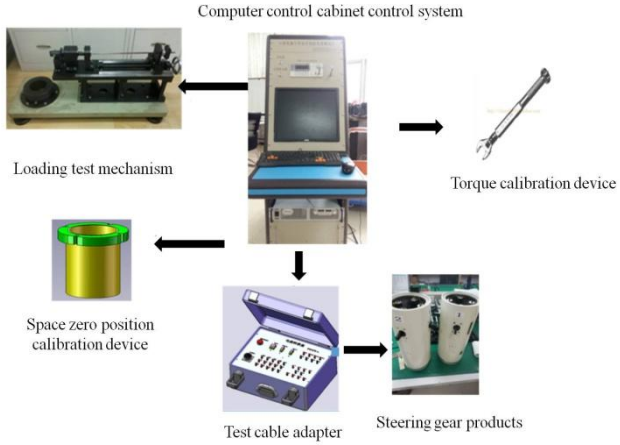

Fig. 13 Steering gear test system

(1) Step-response characteristic test

The step response characteristics include rise time, response time, and overshoot. The input signal adopts two-step signals, the duration of each signal is 1 s, and the amplitude of the signal is 2° and − 2°, respectively, which can calculate the step response characteristics of the tested system in the forward and reverse directions. There is a zero-value signal for 1 s between the two-step signals to ensure that the system is stable before running the step signal. The input and output data curves are shown in Fig. 14. This test directly reflects the rapidity of the positioning of the steering gear.

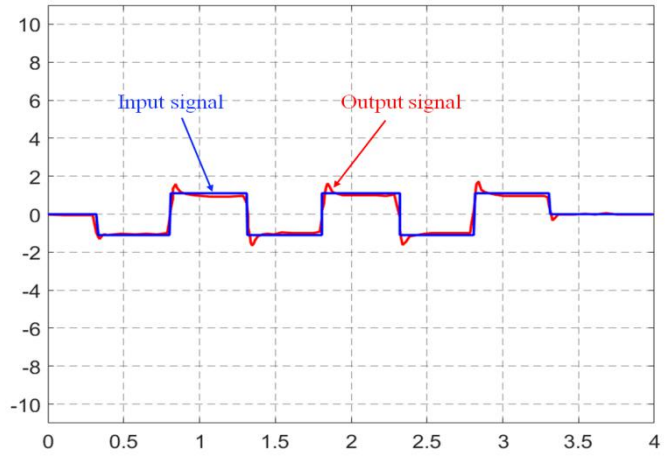

Fig. 14 Step response characteristic input and output data curve

According to the method described above, the rise time is set as the time required for the output value of the system to be 5 % to 95 % of the steady-state value (obtained by calculating the mean value of the stable part), measure the forward and reverse rise times, respectively, and takes the larger value as the result. The average rise time of the tested system is 33.4 ms.

(2) Frequency characteristic test

The frequency characteristic is composed of amplitude and phase frequency characteristics, which can be expressed as amplitude ratio (or amplitude attenuation) and phase difference of the output and input signals, respectively. The amplitude and phase of the input signal at a certain frequency are defined as A_i , and θ_i , respectively, the output signal is defined as A_0 , θ_o respectively, the amplitude frequency characteristic of the tested system at that frequency is, $20\lg(A_0 / A_i)$ and the phase frequency characteristic is θ_0 / θ_i . The sine signal is used as the input signal and tested multiple times. The amplitude of each frequency component was 2°, and the measured frequency range was 1–25Hz. According to the Bode diagram obtained from the collected data fitted by the frequency response method, the amplitude frequency width (-3 dB) of the system is 15 Hz, and the phase frequency width (-90 d) is 75° (Fig. 15). In the fitting process, some line segments are used to approximate the experimental amplitude frequency characteristics, and the frequency inflection point is extracted; thus, there exists some inevitable and small range errors. In conclusion, the transfer function identified by the frequency response method accurately reflects the performance of the actual steering system.

3.3 Transfer function identification of digital actuator control system

The actuator system includes many non-linear links, such as VLDT sensor, power amplifier module, mechanical transmission, and control delay. Therefore, in the process of modeling, linearization is performed in the system mode, thus causing the system to lose information. To establish the mathematical model of the steering system more accurately, the system identification method is used to model the steering system. In this study, the frequency response method is used to identify the steering gear system, and the mathematical model of the steering gear system is established using the Bode diagram obtained from the test. The steering gear test system is composed of a computer test system, steering gear controller, and tested steering gear. The working process is as follows: (1) after the steering gear is powered on, the output terminal of the steering gear is in the zero position. (2) The computer test system sends a sine wave signal with amplitude of 1 V, the sine wave frequency is between 1 Hz to 25 Hz, and the computer test system collects the feedback signal of the steering gear simultaneously. (3) The frequency characteristic test data are collected, as summarized in Table 1, and the Bode diagram of the steering gear system is drawn by the test system, as shown in Fig. 16. It is almost the same as the simulation results of the Bode diagram of the steering gear system (Fig. 11), and verifies the accuracy of the transfer function.

The second-order transfer function of the actuator product was also obtained from the test.

$$G(s) = \frac{1.040188825}{0.00006781194976s^2 + 0.01445985783s + 1} \quad (14)$$

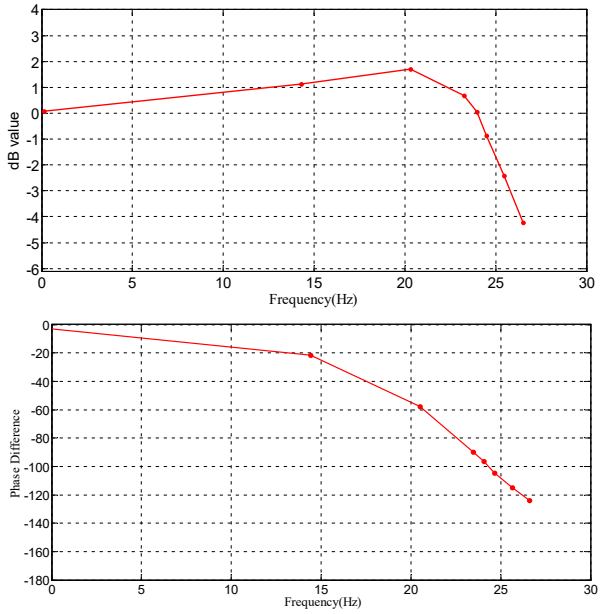

Fig. 15 Measurement results of the steering gear test system with Bode diagram

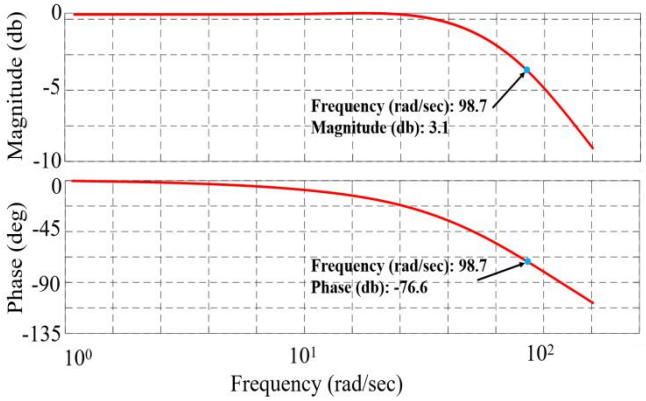

Fig. 16 Bode diagram of the steering gear system

Table 1 Table of amplitude ratio and phase difference at different frequencies

	Frequency	Amplitude ratio (output voltage / input voltage)	Phase difference/°
A	1Hz	1.018984550	-3.130700289
B	2Hz	1.048666697	-7.530035292
C	5Hz	1.063539056	-25.06537523
D	6Hz	1.043156716	-30.90261892
E	8Hz	.9833094698	-41.87360968
F	10Hz	.9068256428	-51.8543718
G	11Hz	.8693040128	-56.1571787
H	12Hz	.8359126236	-60.50736162
I	13Hz	.7976360696	-64.36033160
J	14Hz	.7626966914	-68.22276030
K	15Hz	.7282263824	-72.19244266
L	16Hz	.6916505645	-75.56165285
M	17Hz	.6601947865	-78.83093118
N	18Hz	.6304441114	-82.93651545
O	19Hz	.6013670272	-86.76687829
P	20Hz	.5712003686	-90.37478488
Q	21Hz	.5406026871	-94.32956723
R	22Hz	.5105681367	-99.16135019
S	24Hz	.4345177353	-107.5204676
T	25Hz	.4123836779	-111.1359661

IV. Conclusion

(1). The dynamic mathematical model of the digital steering gear servo control system is established. In this paper, a segmented error PID control method is proposed to analyze the dynamic characteristics of the actuator. The results verify the accuracy of the segmented error PID control method in providing feedback on the dynamic characteristics of the system.

(2). Based on the simulation control model of the digital servo control system, the step response characteristics and frequency characteristics of the prototype servo system were tested. The test results predict the dynamic characteristics of the servo system.

(3). Using the least squares method, the transfer function of the servo system is identified; further, the accuracy of the identification transfer function is verified on comparison with the simulation model.

References

[1]. Wang Qun and Geng Yun Ling, "Electromagnetic gun and its characteristics and military application" , *National Defense Science and Technology*, vol. 32, no. 2, pp. 1-7, 2011.

[2]. Huang Yusen and Zhang Changfan, "The development of electromagnetic railgun and its niche approach" , *National Defense Science and Technology,* vol. 37, no. 3, pp. 33-35, 2016.

[3]. Cui Xiangyang,Li She and Feng Hui, et al, "A triangular prism solid and shell interactive mapping element for electromagnetic sheet metal forming process" , *Journal of Computational Physics,* vol. 27, no. 6, pp. 192-211, 2017.

[4]. Li Zheng You, Xu Zhong and Gao Yushui, "Electric characteristic detection of a certain missile rudder" , *Journal of Academy of Armored Force Engineering,* vol. 12, no. 2, pp. 59-62, 2008.

[5]. He Xiao Hui, "The Research of the Servo Control System of the Electromechanical Actuator" , *Hunan University*, 2015.

[6]. Zhou Weizheng, Li Xuefeng, and Zeng Qinghua, "Research on health simulation and evaluation for electric servo system based on parameter identification" , *Journal of National University of Defense Technology,* vol. 15, no. 8, pp. 132-136, 2016.

[7]. Zhang Jiabao, Liuhui, Jia Hongguang and Xuan Ming "Model identification and corrector design for servo system of electromechanical actuator" , *Optics and Precision Engineering,* vol. 7, no. 16, pp. 1971-1976, 2008.

[8]. Ma Min, Zhou Shengchun, Wang Bobo and Xue Qing, "Parameter identification of electric actuator servo system on aircraft" , *Computer Simulation,* vol. 9, no. 3, pp. 88-93, 2016.

[9]. Wang Xiuyan and Zhang Gewen, "Composite control for electric load simulator based on parameter estimation" , *Drive and Control,* vol. 10, no. 44, pp. 57-61, 2016.

[10]. Sun Yukai, Zhang Renjia and Wu Zhigang, "Dynamic characteristic test and system identification of model rudder" , *Journal of Beijing University of Aeronautics and Astronautics*, vol. 46, no. 2, pp. 294-303, 2020.

[11]. Yang Binyan, Cheng Shencheng Zhu wei and Zhang Tao, "Fault diagnosis of missile electric actuator based on transfer function identification" , *Journal of Naval Academy of Aeronautics and Engineering*, vol. 1, no. 5, pp. 494-498, 2012.

[12]. Zhang Jiabo, Liu Hui, Jia Hong guang and Xuan Ming, "Model identification and correction of servo system of electric actuator" , *Optical Precision Engineering*, vol. 12, no. 10, pp. 185-190, 2008.

[13]. Wu Zhihong， Yang Ruifeng and Guo Chenxia, "Steering system identification based on improved adaptive genetic algorithm" , *Science Technology and Engineering*, vol. 20, no. 11, pp. 4436-4441, 2020.

[14]. Maarif A , Cahyadi A I , Herdjunanto S, Iswanto I and Yamamoto Y, "Tracking control of higher order reference signal using integrators and state feedback" , *IAENG Internaitonal Journal of Computer Science*, vol. 46, no. 2, pp. 208-216, 2019.

[15]. Kharchenko O I, "Modeling nonlinear stochastic filter by volterra transfer functions" , *Engineering Letters,* vol. 28, no 2, pp. 262-267, 2020.

[16]. Zhong Y T, "Design of servo control test and analysis system" , *Hua Zhong University of Science and Technology*, 2007.

[17]. Deng Hongyang and Doroslovacki M, "Improving convergence of the PNLMS algorithm for sparse impulse response identification" , *IEEE Signal Processing Letters*, vol. 12, no 3, pp. 181-184, 2005.

[18]. Ahmed S, "Step response-based identification of fractional order time delay models*" , Circuits, Systems, and Signal Processing*, vol. 8, no 6, pp. 1-17, 2020.

[19]. Li Feng and Li Jia, "Correlation analysis-based error compensation recursive least-square identification method for the Hammerstein model," *Journal of Statal Computation and Simulation,* vol. 88, no 3, pp. 56-74, 2018.

[20]. Liu Lijuan, Ding Feng and Hayat T, "Maximum likelihood gradient identification for multivariate equation-error moving average systems using the multi-innovation theory" , *International Journal of Adaptive Control and Signal Processing,* vol. 33, no 7, pp. 1031-1046, 2019.

[21]. Ding Feng, Liu Guangjun and Liu Xiaoping, "Partially coupled stochastic gradient identification methods for non-uniformly sampled systems" , *IEEE Transactions on Automatic Control*, vol. 55, no 8, pp. 1976-1981, 2010.

[22]. Ding Feng and Chen Tongwen, "Performance analysis of multi-innovation gradient type identification methods" , *Automatica*, vol. 43, no 1, pp. 1-14, 2007.

[23]. Ding Feng and Chen Tongwen, "Hierarchical identification of lifted state-space models for general dual-rate systems" , *IEEE Transactions on Circuits & Systems I Regular Papers,* vol. 52, no 6, pp. 1179-1187, 2005.

[24]. Wu Xuhui and Tang Tao, "Research on the application of PID control algorithm with variable coefficient in servo system" , *Automation and Instrumentation,* vol. 8, no 4, pp. 18-19, 2016.

[25]. Tang Jia, Liu Shiqi and Liu Jingwen, "Charge discharge parameter identification of urban rail train energy storage components based on vector multi forgetting factor least square method" , *Journal of Wuhan University (Engineering Edition),* vol. 53, no 6, pp. 527-533, 2020.

[26]. Li Wanjun and Li Guangyang, "The correction of steering gear monitoring and control parameters based on the method of least squares" , *Techniques of Automation and Applications*, vol. 8, no 751, pp. 631-632, 2014.

[27]. Ding Feng. System identification, "Part C: Identification accuracy and basic problems" , *Journal of Nanjing University of Information Science and Technology: Natural Science Edition*, vol. 3, no 3, pp. 193-226, 2011.

[28]. Ding Feng and Ding Tao, "Convergence of least squares identification under attenuating excitation condition for stochastic systems" , *Journal of Hubei Polytechnic University,* vol. 16, no 1, pp. 5-7, 2001.